

# We are IntechOpen, the world's leading publisher of Open Access books Built by scientists, for scientists

6,900

Open access books available

186,000

International authors and editors

200M

Downloads

Our authors are among the

154

Countries delivered to

TOP 1%

most cited scientists

12.2%

Contributors from top 500 universities



WEB OF SCIENCE™

Selection of our books indexed in the Book Citation Index  
in Web of Science™ Core Collection (BKCI)

Interested in publishing with us?  
Contact [book.department@intechopen.com](mailto:book.department@intechopen.com)

Numbers displayed above are based on latest data collected.  
For more information visit [www.intechopen.com](http://www.intechopen.com)



---

# Review on Microwave Metamaterial Structures for Near-Field Imaging

---

Hatem El Matbouly

Additional information is available at the end of the chapter

<http://dx.doi.org/10.5772/66831>

---

## Abstract

In the past decade, metamaterials have attracted a lot of attention because of their abilities to exhibit unusual electromagnetic properties. These properties are exploited in designing functional components and devices for many potential applications. In this chapter, we review the theory and design of metamaterial structures for microwave near-field imaging/microscopy. The chapter highlights metamaterial microwave components to obtain super-resolution and manipulating subwavelength images. Moreover, a review on surface plasmons manipulation at microwave frequencies is presented as a technique to enhance the transmission for near-field microscopy. The chapter presents as well a survey on the near-field imaging instrumentation and its advances mainly for microwave and THz regimes.

**Keywords:** metamaterials, microscopy, near-field, microwave, novel electromagnetic structures, subwavelength imaging, surface plasmons

---

## 1. Introduction

The technique of microwave near-field microscopy is used to characterize materials by measuring the microwave electromagnetic response of materials on length scales shorter than the wavelength of the incident electromagnetic wave. With this technique one can achieve a spatial resolution at a submicrometer level compared to conventional far-field imaging technique, which has a resolution limitation [1]. This technique may facilitate new measurements on systems that cannot be studied directly with scanned probes, such as buried features or single molecule detection [2] as well as in biomedical applications [3].

New advances in metamaterials research are making unnatural electromagnetic phenomena become realizable [4]. The purpose of this chapter is to focus on using metamaterial and its exciting properties for the enhancement of near-field microscopy and imaging.

---

This chapter starts with a general overview on the near-field imaging/microscopy and its applications including a description of the microwave near-field imaging system and its components. Metamaterial design technique will be discussed as a step to design novel structures that allow further improvements in spatial resolution.

The chapter concludes with a review on another possibility to enhance microwave near-field microscopy that is the manipulation of surface plasmons at microwave and millimeter-wave frequencies. This can enhance the transmission through subwavelength near-field apertures.

## 2. Overview on microwave near-field imaging/microscopy

### 2.1. Backgrounds

The conventional far-field optical imaging system suffers from resolution limitations, this is due to Abbe's theory that restrains the spatial resolution to a diffraction limit [5]. In case of far-field imaging, forming an image is subjected to the Rayleigh criterion, which is the condition to resolve the diffraction pattern of two points separated by a distance of  $\Delta y$ . This condition is given by  $\Delta y = 0.61 \lambda/\text{NA}$ , where  $\lambda$  is the wavelength and (NA) is the numerical aperture of the microscope [6]. On the contrary, subwavelength spatial resolution imaging can only be achieved by using near-field technique suggested first by E.A Synge in early 1928 (see the next section for a survey on near-field technique). The near-field results in the excitation of an electric dipole moment within a sample, the idea is to probe the dipole radiation in the near-field region,  $\vec{E}_{rad}$  is the radiated electric field and  $\vec{B}_{rad}$  is the radiated magnetic field of the dipole radiation which are given by [7]

$$\vec{E}_{rad} = \frac{1}{4\pi\epsilon_0} \left\{ k^2 (\hat{r} \times \vec{p}) \times \hat{r} \frac{e^{ikr-\omega t}}{r} + (3r(\hat{r} \cdot \vec{p}) - \vec{p}) \left( \frac{1}{r^3} - \frac{ik}{r^2} \right) e^{ikr-\omega t} \right\} \quad (1)$$

$$\vec{B}_{rad} = \frac{1}{4\pi} \left\{ k^2 (\hat{r} \times \vec{p}) \left( \frac{1}{r^3} - \frac{ik}{r^2} \right) e^{ikr-\omega t} \right\} \quad (2)$$

where  $\vec{p}$  is the dipole moment,  $k$  is the wave number and  $\vec{r}$  is the distance between the source and the observation point. The first part of Eq. (1) is the propagating far field of the dipole radiation that cannot be used for subwavelength imaging because the diffraction limits the image resolution. However, the second part is the near field of the dipole radiation and there is no diffraction problem associated with using it since it has a nonpropagating nature. In this case the spatial resolution will not be limited by the wavelength if the nonpropagating near field is used [7, 8].

### 2.2. Description of a microwave near-field imaging microscope

A schematic diagram of the near-field microwave microscope is shown in **Figure 1**. The near-field microscope consists of a microwave source, a transmission line resonator coupled to the

microwave generator, a near-field probe connected to the transmission line, a detector to measure the reflected signal from the resonator and a feedback circuit [9].

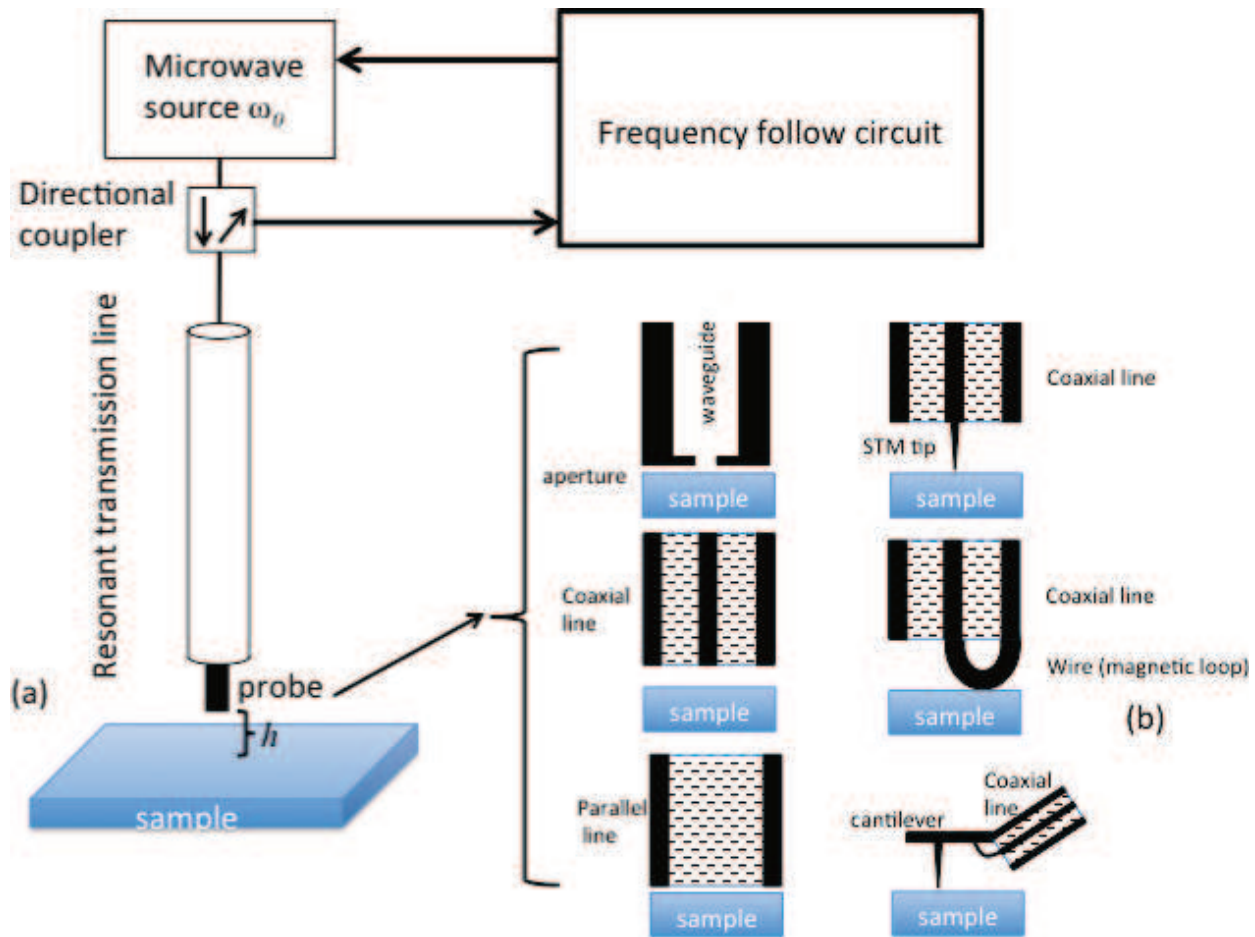


**Figure 1.** The schematic diagram of the near field microscope (a) the structure of the microscope and (b) different near field probe structures.

The probe is an antenna-like structure operating at the subwavelength, which is used to scan in close proximity of the sample's surface. As shown in **Figure 1(a)**, the probe can take different forms for instance it can be an aperture in an opaque screen, an electric wire formed by a sharpened rod or scanning tunneling microscopy (STM) tip, an atomic force microscopy (AFM) tip, an electrically open flush end of a transmission line, a magnetic loop, or a variety of other geometries [10]. The electromagnetic response of the surface is measured as the probe is scanned over the sample [11]. The probe can be either in contact or at a separation  $h$  from the sample surface, which is usually much less than the probe characteristic length-scale  $D$ , this ensures a good signal level from the sample surface [11, 12]. In the near zone of an antenna, the structure of electric and magnetic fields is more complicated as their distribution is strongly dependent on the antenna geometry as well as electrodynamic properties of the surrounding region [13–15].

The design of near-field probes can be divided into two main categories, aperture-based probes and apertureless probes [16]. For aperture-based probes, a subwavelength aperture is

used to limit the illuminating source, or to collect the local near-field response. It can be a subwavelength hole in a metallic film, a metallic coated pipette, or a tapered optical fiber as illustrated in **Figure 1(b)**.

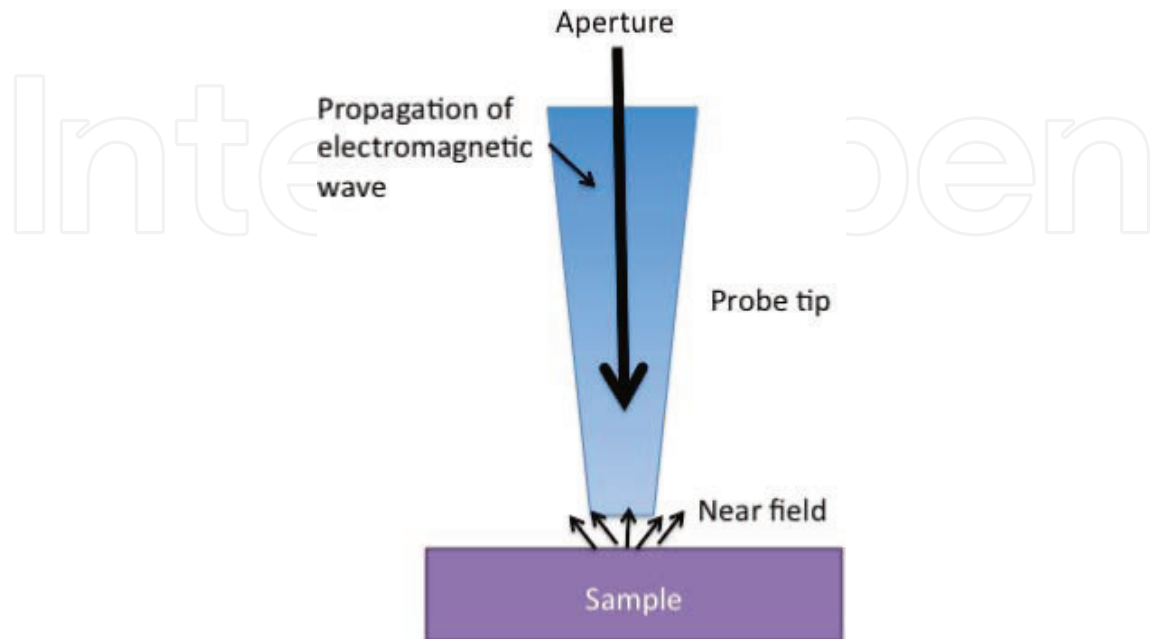


**Figure 1 (b).** Near-field imaging using aperture type probe.

By positioning the aperture in the close proximity of the sample, the transmitted wave through the aperture only represents the local properties of the sample. Thus, in principle, subwavelength spatial resolution becomes possible by reducing the aperture size and raster scanning the sample surface [17]. The concept was first experimentally demonstrated by Ash and Nicholls [26] (see the next section for a survey on near-field technique), who resolved a  $\lambda/60$  grating structure by using  $\lambda = 3$  cm microwave (10 GHz). In optical frequencies, the spatial resolutions are typically tens of nanometers when using a tapered single mode optical fiber probe. However, the aperture probes suffer from strong signal attenuation. For a hole in a metallic film, the electric field transmission is proportional to  $(D/\lambda)^3$ , where  $D$  is the diameter of the hole [11, 13]. For an optical fiber probe, the image contrast suffers from a strong decrease when the aperture diameter exceeds a critical value. So the signal intensity will be far too small to be detected when the aperture size is further reduced to achieve a better spatial resolution. On the other hand, for the long wavelength of THz radiation, according to the wavelength dependence, the transmission efficiency is extremely low and makes the THz aperture near-field imaging impractical.

An alternative approach is to allow a propagating wave to irradiate some large portion of the sample, but to employ a field-concentrating feature, such as a tip, to enhance the probe-sample interaction locally. **Figure 2** shows the probing using apertureless near-field probe.

Using a metallic probing tip, the incident wave is scattered by the tip-surface system. Usually, the scattering wave is modulated by a dithering tip and measured in nonspecular directions due to reduced background noise. The wave scattering depends on the local surface

properties. By measuring the scattering wave when scanning over a sample, the surface properties can be mapped. In principle, the spatial resolution for an apertureless probe is only limited by the size of the probing tip. Resolution as small as 10 angstrom has been reported with this technique at optical frequencies and a subwavelength factor of  $10^{-6}$  was achieved at the microwave region [18].

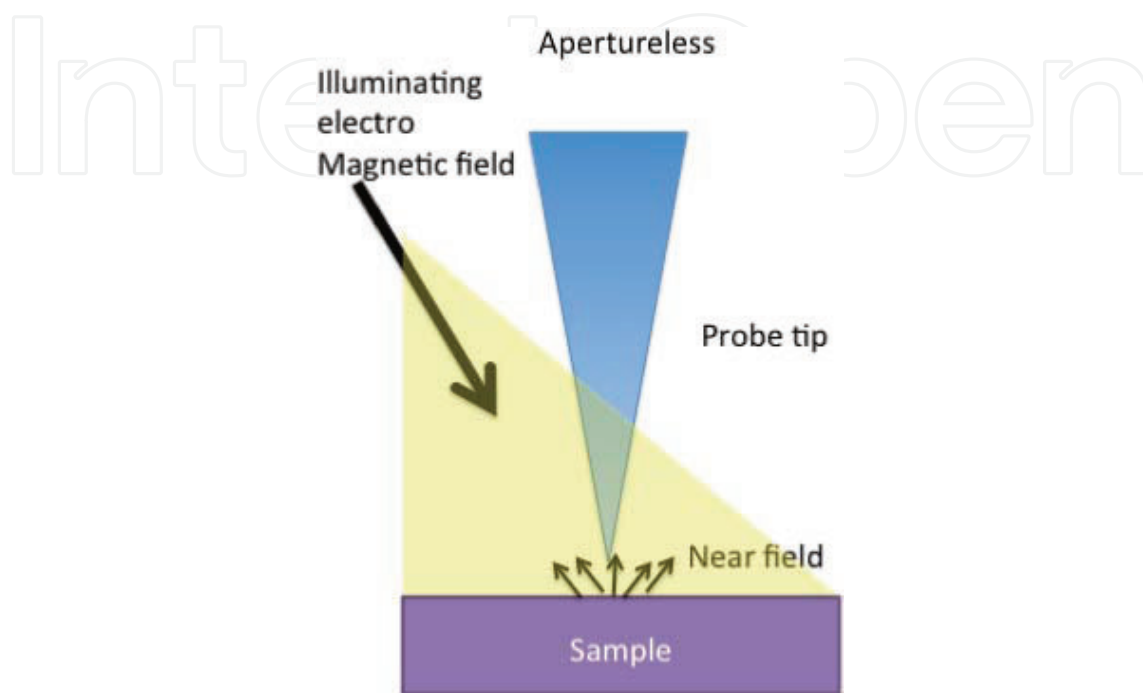


Figure 2. Near-field imaging using apertureless type probe.

### 3. Survey on near-field imaging from microwave to terahertz frequencies

The idea of near-field microscopy was first demonstrated theoretically by Synge in 1928 [19]. He used an opaque screen with a small subwavelength diameter hole (10 nm in diameter) at 10 nm above the surface of an optically transparent flat sample. The transmitted light is collected by raster scanning the surface. Detailed calculations of the near-field distribution of an aperture were conducted later by Bethe [20] and Bouwkamp [21, 22]. A large fraction of high-spatial frequency evanescent waves is contained in the near field, which can lead to subwavelength spatial resolution [23, 24].

In the 1960s, when the idea of near-field imaging transferred to practice, ferromagnetic resonance microwave microscopy has been developed to characterize ferromagnetic material thin films, for example, Soohoo developed a microwave magnetic probe capable of measuring the spatial variation of the magnetic properties of materials [25] using a cavity made of superconducting material.

A detection system using quasi-optical hemispherical resonator was used at microwave frequencies by Ash and Nicholls [26]. In this experiment, a small aperture (1.5 mm diameter) similar to Synge geometry is used. The aperture is scanned over a sample with a microwave

signal at 10 GHz. The sample was harmonically distance modulated at a fixed frequency and the reflected signal was phase-sensitively detected at this modulation frequency to improve sensitivity to sample contrast. This microscope demonstrated contrast sensitivity to metal films on dielectric substrates, as well as bulk dielectrics with dielectric constant differing by only about 10%.

Nonresonant scanned aperture probes were also developed in the 1960s. In the case of nonresonant probe, a transmission line (coaxial or waveguide) delivers a microwave signal to the probe aperture where the fringe electric and magnetic fields from the aperture interact with the sample. Some part of the signal is stored locally in evanescent and near-zone waves, some is absorbed by the sample, some is reflected back up the transmission line and some is scattered away as far-field radiation. By monitoring the scattered or reflected signals as a function of probe height and position, an image of the sample response can be constructed. An example of this type of probe was developed by Bryant and Gunn [27]. They measured the reflected signal from a tapered open-ended coaxial probe with an inner conductor diameter of 1 mm. The probe was used for quantitative measurements of semiconductor resistivities between 0.1 and 100  $\Omega \text{ cm}^{-1}$ .

The development of near-field optical microscopes using optical waveguides beyond cutoff [28, 29] affected the development of new microwave microscopes. The first of these microwave systems operating at 2.5 GHz was developed by Fee et al. to measure the reflected signal from a nonresonant open-ended coaxial probe [30]. A 500- $\mu\text{m}$  in diameter conductor coaxial probe is used and the central conductor was sharpened to a tip of 30  $\mu\text{m}$  in radius. An image of copper grid lines showed a spatial resolution of about 30  $\mu\text{m}$  (or  $\lambda/4000$ ). Other waveguide structure microscopes based on a scanned aperture were developed by Golosovsky et al. [31, 32] and Bae et al. [33–35].

The first THz near-field microscopy was demonstrated in [36]. In this work, a tapered metallic waveguide was used as the aperture to limit the size of the incident ultrashort THz pulses. The probe aperture is similar to the tapered optical fiber tips used in most of scanning near-field optical microscopy. With the aperture diameter  $\sim \lambda/3$  (100  $\mu\text{m}$ ), a spatial resolution better than  $\lambda/4$  was demonstrated for a gold pattern on silicon substrate. A collection mode THz scanning near-field microscopy was developed by Mitrofanov et al. [37–39]. It uses an aperture-type probe to collect the near field instead to filter the illuminating light. He showed improvements in sensitivity and resolution by integrating the probe and a photo-conducting antenna THz detector in the near-field region of the aperture. THz near-field imaging with a dynamic aperture was demonstrated by Wynne et al. and Chen et al. [40, 41]. In his work, the dynamic aperture was formed by a transient photo-carrier layer induced by a THz near-field imaging. In case that the optical pulse arrives earlier than the THz pulse, the THz transmission is modulated by the induced photo-carrier layer, whose size is determined only by the optical beam focus. This approach has the potential to improve spatial resolution and image contrast, while it is limited to semiconductor surface.

Apertureless THz near-field imaging has been also investigated [42, 43]. In their work, van and Planken used a metallic probing tip with THz waves to image down to 18  $\mu\text{m}$  in size. Moreover, a scattering type apertureless THz scanning near-field microscope has been

demonstrated by Wang et al. [44]. THz radiation is scattered and modulated by the dithering metallic probing tip in the tip-surface system, the THz signal is detected in nonspecular directions [45].

## 4. Metamaterial for near-field imaging manipulation

Conventional imaging devices or lenses suffer from diffraction limit which constrain the image resolution. In addition, conventional imaging cannot propagate the evanescent waves which carry the subwavelength information due to the exponential decay exhibited in natural materials. These issues can be overcome using metamaterials. For instance, image focusing, rotation, lateral shift and image magnification are achievable with subwavelength resolutions using a two- or three-dimensional metamaterials structures, usually with negative refraction properties, to achieve resolution beyond the diffraction limit (ideally, infinite resolution). Such behavior is enabled by the capability of double-negative materials to yield negative phase velocity.

### 4.1. Metamaterial design by electromagnetic field transformation

Electromagnetic metamaterials are periodic structures that can artificially manipulate the electromagnetic properties of media. They can be engineered for the radio-frequency (RF) and microwave range as well as for terahertz and optical frequencies. Metamaterials allow the possibility of attaining mediums with properties, which have not been considered before, such as, negative or close to zero refractive index since they are inaccessible in nature. In addition, they can mix the electric and magnetic response of a material (chirality) [46, 47]. The first step to design a metamaterial medium is using the electromagnetic transformation to get the new medium properties (i.e., transformed permittivity and permeability). Transformation electromagnetics are based on the invariance of Maxwell's equations with respect to coordinate transformations; this enables a user-defined coordinate transformation to be translated into electric and magnetic material parameters. **Figure 3** shows the relations between the different coordinates [48, 49].

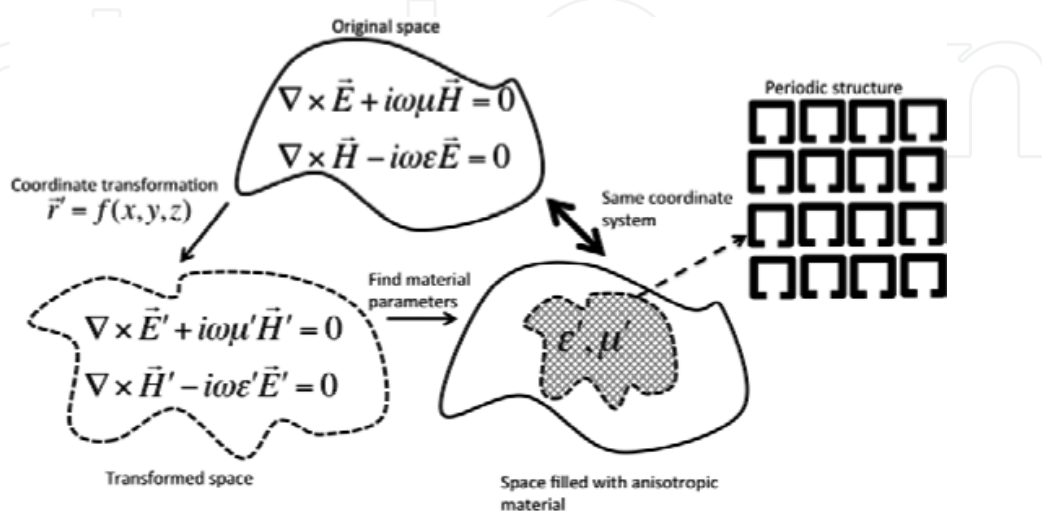


**Figure 3.** Transformation electromagnetic for metamaterial medium.

Once the transformed permittivity and permeability and their spatial distribution are obtained, the structure of unit cell (or particle) is designed by optimizing its geometric parameters. The most common unit cell structure is the split ring resonator (SRR). The unit cell can be a resonant or nonresonant. In case of the resonant unit cell, the losses are high at the resonance frequency; however, they have a large dynamic rang. The nonresonant unit cell has the advantage of small losses but with low dynamic rang [49].

#### 4.2. Metamaterials medium types

The electromagnetic mediums are categorized as isotropic or anisotropic. In the isotropic electromagnetic medium the permittivity,  $\epsilon$  and permeability,  $\mu$ , of the medium are uniform in all directions of the medium. The dispersion relation in that medium is  $k = \omega\sqrt{\mu\epsilon}$ . One simple example of an isotropic electromagnetic medium is the free space. However, the medium is called anisotropic when the permittivity,  $\epsilon$  and permeability,  $\mu$ , of a medium depend upon the directions of field vectors and hence, they are in tensor form. Based on Maxwell equations in an anisotropic medium the dispersion relation can be obtained by solving the matrix equation [49, 50]:

$$\det[\bar{k} \cdot \bar{\epsilon}^{-1} \cdot \bar{k} + k_0^2 \bar{\mu}] = 0 \quad (3)$$

where  $\bar{\mu}$ ,  $\bar{\epsilon}$  and  $\bar{k}$  are all matrices and  $k_0^2 = \omega^2 \mu_0 \epsilon_0$  ( $\mu_0, \epsilon_0$  are the permeability and permittivity of free space, respectively). Metamaterials are composite structures in which the electromagnetic wave propagation depends on the orientation of structured metallic unit cells. Usually, these unit cells are designed to have a certain permittivity and permeability responses by optimizing its geometric parameters. One common example of unit cell structure is the split ring resonator (SRR) (see Section 4.1) [51]. The anisotropic metamaterial is defined with its permittivity and permeability tensor as follows

$$\bar{\epsilon} = \begin{pmatrix} \epsilon_x & 0 & 0 \\ 0 & \epsilon_y & 0 \\ 0 & 0 & \epsilon_z \end{pmatrix} \text{ and } \bar{\mu} = \begin{pmatrix} \mu_x & 0 & 0 \\ 0 & \mu_y & 0 \\ 0 & 0 & \mu_z \end{pmatrix} \quad (4)$$

where the diagonal elements of  $\bar{\epsilon}$  and  $\bar{\mu}$  could have positive or negative values. To understand the propagation properties of a wave in such medium a TE plane wave is considered. Using Eqs. (3) and (4), one can get the anisotropic dispersion relation of the medium

$$\frac{k_y^2}{\epsilon_z \mu_x} + \frac{k_x^2}{\epsilon_z \mu_y} = \frac{\omega^2}{c^2} \quad (5)$$

where  $c$  is the speed of light in free space and  $k$  is the wave vector of the propagating wave. For losses material, the plane wave solution in the anisotropic medium can be either a propagating wave or evanescent wave depending on the sign of the wave number  $k_x$  and hence, the medium can be classified as in **Table 1** [49].

Medium type	Material parameters	Wave property	Cut off conditions
Cutoff media	$\epsilon_z \mu_y > 0, \frac{\mu_y}{\mu_x} > 0$	Propagating	$k_y < k_c$
		Evanescient	$k_y \geq k_c$
Anti-cutoff media	$\epsilon_z \mu_y < 0, \frac{\mu_y}{\mu_x} < 0$	Evanescient	$k_y < k_c$
		Propagating	$k_y \geq k_c$
Never-cutoff media	$\epsilon_z \mu_y > 0, \frac{\mu_y}{\mu_x} < 0$	Propagating	All real $k_y$
Always-cutoff media	$\epsilon_z \mu_y < 0, \frac{\mu_y}{\mu_x} < 0$	Evanescient	No real $k_y$

**Table 1.** Anisotropic media for a z-polarized TE plane wave.

### 4.3. Construction of compensated bilayer of anisotropic metamaterials for imaging

Veselago introduced the bilayer compensation to illustrate the ability to focus on the electromagnetic wave from a point source by a flat slab of composite material with a negative refraction. The proposed structure was a bilayer of vacuum and a left-hand material (with permittivity and permeability equal to  $-1$ ) where the left-hand material compensates for the propagation effect associated with an equal length of vacuum. This bilayer structure is called Veselago lens (or the perfect lens) [52]. The same idea can be implemented using positive and negative refracting layers of anisotropic metamaterials to implement near-field focusing in the same way as Veselago lens. **Figure 4** shows the bilayer of anisotropic metamaterials in two dimensions.

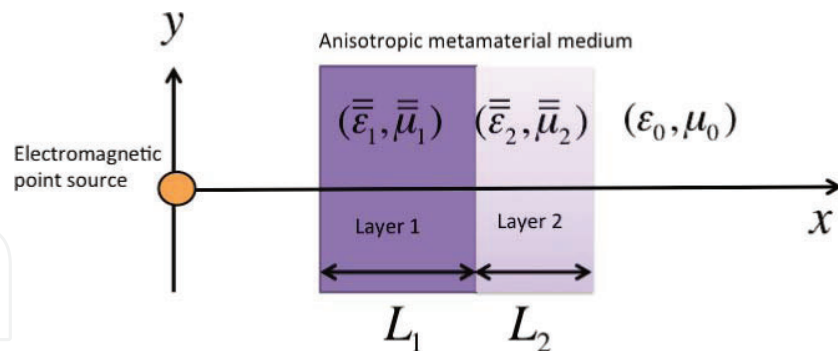


**Figure 4.** Compensated anisotropic metamaterial medium structure.

Depending on the sign of the permittivity and permeability of the two layers, one can get different material types for the compensated bilayers. For instance, compensated bilayer can be made of combination of positive and negative refracting layers of never-cut off medium (NCM) or anticutoff medium (ACM). **Table 2** shows examples of metamaterials that could make up the compensated bilayer [49].

Bilayer type	Layer	$\epsilon_x$	$\epsilon_y$	$\epsilon_z$	$\mu_x$	$\mu_y$	$\mu_z$	Material
Veselago lens	L1	1	1	1	1	1	1	Free space
	L2	-1	-1	-1	-1	-1	-1	Left hand material
NCM compensated bilayer	L1	-1	1	1	-1	1	1	Positive refractive NCM
	L2	1	-1	-1	1	-1	-1	Negative refractive NCM
ACM compensated bilayer	L1	1	-1	-1	-1	1	1	Positive refractive ACM
	L2	-1	-1	1	1	-1	-1	Negative refractive ACM

**Table 2.** Compensated bilayer anisotropic metamaterial types.

## 5. Near-field subwavelength image manipulating through compensated anisotropic metamaterial

### 5.1. Superlens

As mentioned earlier, the performance limitation of conventional lenses is due to the diffraction limit. In conventional imaging the field emitting from an object is a superposition of plane waves with dispersion relation given by [53]

$$k_z = \sqrt{\frac{\omega^2}{c^2} - (k_x^2 + k_y^2)} \quad (6)$$

In case of energy propagation in the +z-direction, the only real values are the ones allowed for and hence all the components of  $k_z$  contains the spectrum of the image which are transmitted and refocused by an ordinary lens. On the other hand, if  $k_z$  is imaginary, i.e.,  $\frac{\omega^2}{c^2} < (k_x^2 + k_y^2)$ , the wave is an evanescent wave whose amplitude decays as the wave propagates along the z-axis. This leads to a loss of the high-frequency components of the wave, which contain information about subwavelength features of the object being imaged. The super lens with negative-index materials can overcome this problem. Since in such materials transporting the electromagnetic energy in the +z-direction requires negative wave vector. This amplifies the evanescent wave and all components of the angular spectrum can be transmitted without distortion [53].

Super lensing can be achieved with bilayer of anisotropic metamaterial, i.e., (NCM) and (ACM) bilayers. However, the mechanism of constructing perfect image with subdiffraction resolution in the case of (NCM) and (ACM) bilayers is different than the mechanism of super lens with single-negative index layer (Veselago lens). As discussed in the previous section, the subwavelength resolution, in case of perfect lens, is achieved through the amplification of the evanescent wave which by consequence recovers the subwavelength features. In the case of NCM or ACM bilayers lens, the evanescent components of the wave are converted to a propagating mode in the bilayer region and then back to evanescent component at the back surface of the bilayer which creates an image beyond the

diffraction limit. A comparison between the evanescent wave propagation in different bilayers is shown in **Figure 5** [49, 54].

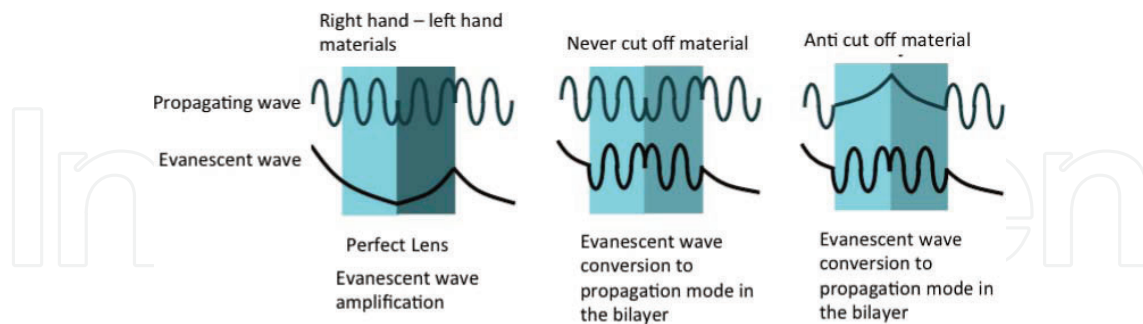


**Figure 5.** Different evanescent wave propagation in three types of metamaterial bilayer structures.

It is important to mention that the electric or magnetic loss is considered a major problem in the implementation of metamaterials in the imaging structures. The reason is that these losses can limit the resolution of the perfect lens. These losses are due to the imaginary part of the permittivity and permeability tensors. In general, the beamwidth of the electric field is degraded at the back surface due to losses compared to the source plane. The effect of degradation is different depending on the type of the bilayer used for the super lens. In case of the left-hand material lens the electric field degradation is about  $\lambda/5$  while for NCM or ACM is  $\lambda/10$ . This indicates that the NCM and ACM lenses are less sensitive to material parameters losses than the left-hand material lens [49, 55, 56].

Another issue with the bilayer structures is the retardation effect. This effect is due to the difficulty to realize a completely compensated bilayer in practical cases. As with the losses, the retardation effect degrades the electric field beamwidth and the NCM or ACM are less sensitive to that degradation than the left-hand material. This is why anisotropic metamaterial medium is considered advantageous since it can approximate the ideal situation [49, 57].

## 5.2. Bilayer lens using transmission line metamaterial

The bilayer of anisotropic metamaterial for imaging can be realized using L-C transmission line network. Different types of anisotropic metamaterials such as ACM and NCM can be constructed by L-C loaded microstrip line grids operating at certain frequency bandwidth. The planner microstrips are periodically loaded by serial capacitance in  $z$ - or  $y$ -direction with or without shunting inductance loaded at the center of the node. The unit cell of the planner transmission line metamaterial is illustrated in **Figure 6** [47, 49, 58].

For  $z$ -polarized electromagnetic wave the dispersion relation is dependent on  $\epsilon_z$ ,  $\mu_x$  and  $\mu_y$  as indicated in Eq. (5). Dispersion relation of a transmission line metamaterial can be obtained using periodic transmission line theory [59, 60]. For example, under the effective medium approximation, the dispersion relation of the unit cell, shown in **Figure 6(a)**, is

$$\frac{k_y^2}{2\beta^2(1-2\omega_0/\omega\beta d)} + \frac{k_x^2}{2\beta^2} = 1 \tag{7}$$

where  $\omega_0 = 1/2C_y Z_0$ ,  $Z_0$ ,  $\beta$  and  $d$  are the characteristic impedance, the propagation constant and the length of the transmission line section.

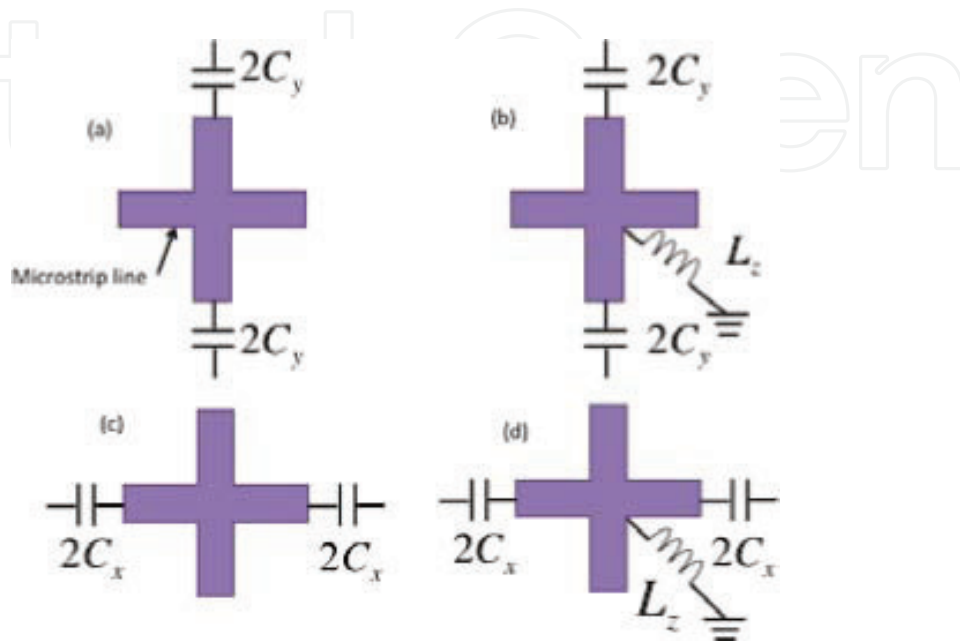


**Figure 6.** Different unit cells of loaded transmission line grid for implementing different anisotropic metamaterials. (a) positive refraction NCM (b) positive refraction ACM (c) negative refraction ACM (d) negative refraction NCM.

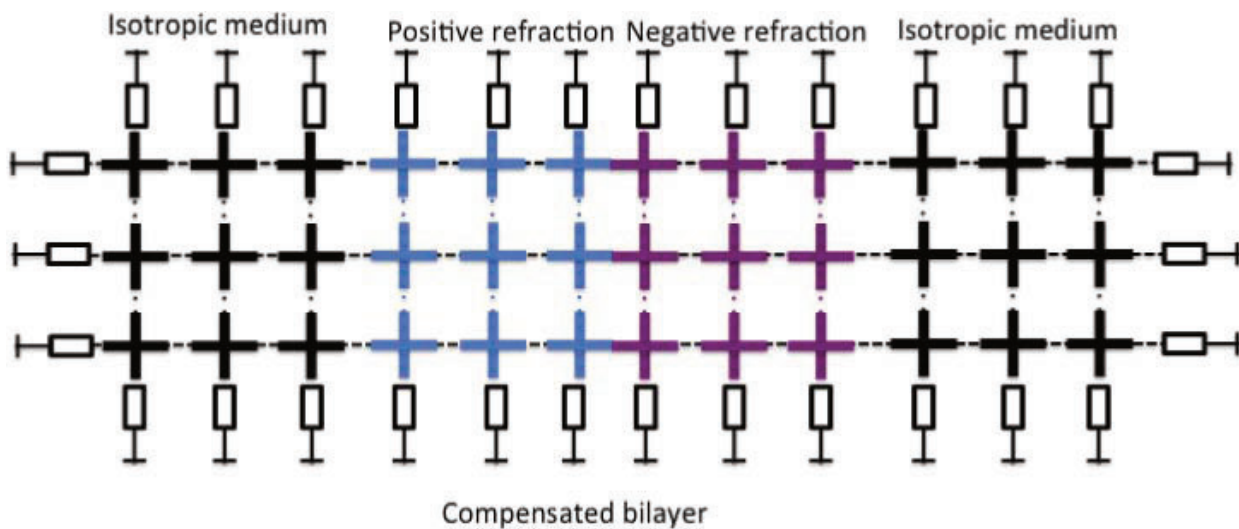


**Figure 7.** The schematic diagram of a 2D compensated bilayer using loaded L-C metamaterial transmission line.

Using these four unit cells in a network, one can construct a 2D compensated bilayer lens composed of positive NCM/negative NCM or positive ACM/negative ACM. **Figure 7** shows

the schematic diagram of the bilayer medium. The loaded capacitances and inductances need to be chosen to satisfy the requirement of the bilayer medium see **Table 2**.

The imaging properties of the compensated bilayer structure are investigated experimentally in the microwave range [61]. The results show that the electromagnetic wave from a point source has been focused on the image plane with beamwidth of  $0.1 \lambda$  which is below the diffraction limit. This focusing result is well below the left-hand material planer lens, which is  $0.21 \lambda$  [49, 61]. The NCM bilayer lens has better subwavelength resolution because it is less sensitive to material losses.

## 6. Plasmonic and field enhancement metamaterials

The structures presented in the previous section such as bilayers and superlens can be integrated in the system of a near-field microwave microscope [62]. This can improve image measurements by improving spatial resolution, this helps in studying surfaces that cannot be imaged directly with a scanned probes. Moreover, the technique of manipulation of surface plasmons for enhancing electromagnetic propagation can be used in imaging system at microwave frequencies. Surface plasmons are known in optical frequency [63]. They can be excited on a metal by an external plane-wave beam. This can enhance the electric field at the surface compared with that in the incident beam and it has been suggested that this effect is an important aspect of surface-enhanced Raman scattering [64]. Surface plasmons have been investigated for extraordinary optical transmission through subwavelength hole arrays [65]. This overcomes the constraint of low transmittivity of subwavelength apertures. Ebbesen et al. observed that the maxima the transmission efficiency could exceed unity (when normalized to the area of the holes), which are orders of magnitude greater than predicted by standard aperture theory [65]. A review that summarizes the basic principles and achievements in the field of plasmonic for subwavelength guiding has been presented [66]. This review chapter discusses as well the potential future developments and applications of nanophotonic devices and circuits and near-field microscopy with nanoscale resolution [67].

Manipulating surface plasmons at microwave and millimeter-wave frequencies is possible due to the field of metamaterials [68]. This can be achieved using composite dielectric where the property of having negative permittivity below the plasma frequency has been investigated [69]. This investigation showed that thin wires structure reduces the plasma frequency having longer wavelength to be diffracted and the system can be described by an effective dielectric constant of the plasma form. This achievement opens new possibilities for microwave structures to produce enhanced transmission through subwavelength apertures as in the case of photonic structures.

## 7. Conclusion

This chapter introduced a review on metamaterial structures for near-field microscopy. A general overview on the near-field imaging/microscopy instrumentation is first presented

followed by a survey on the research done on this topic. The metamaterial design based on transformation electromagnetic as well as a summary on metamaterial media was introduced. The bilayer metamaterial medium is discussed for super-resolution structures that can manipulate subwavelength images and evanescent waves. Finally, the manipulation of surface plasmons is presented as a technique to enhance the transmission for near-field microscopy.

## Author details

Hatem El Matbouly

Address all correspondence to: [hatem.el-matbouly@lcis.grenoble-inp.fr](mailto:hatem.el-matbouly@lcis.grenoble-inp.fr)

LCIS, Grenoble-INP, Grenoble Alpes University, Valence, France

## References

- [1] Eric B, Jay KT, "Near-field optics: microscopy, spectroscopy and surface modification beyond the diffraction limit", *Science*, Vol. 257, No. 5067, pp. 189–195, 1992.
- [2] Xiaoliang SX, Robert CD, "Probing single molecule dynamics", *Science, New Series*, Vol. 265, No. 5170, pp. 361–364, 1994.
- [3] Chen H, Ma S, Wu X, Yang W, Zhao T, "Diagnose human colonic tissues by terahertz near-field imaging", *Journal of Biomedical Optics*, Vol. 20, No. 3, art. no. 036017, 2015.
- [4] Yuandan D, Tatsuo I, "Promising future of metamaterials", *IEEE Microwave Magazine*, March, 2012.
- [5] Born M, Wolf E, "Principles of optics", Cambridge University Press, Cambridge, 6th edition, 1998.
- [6] <http://hyperphysics.phy-astr.gsu.edu/hbase/phyopt/raylei.html>
- [7] Jackson J, "Classical Electrodynamics", John Wiley, New York, 3rd edition, 1998.
- [8] Alexander NR, Nadezhda VY, "Electrodynamics of microwave near-field probing: Application to medical diagnostics", *Journal of Applied Physics*, Vol. 98, art. no. 114701, 2005.
- [9] Steven MA, Steinhauer DE, Feenstra BJ, Vlahacos CP, Wellstood FC, "Near Field Microwave Microscopy of Materials Properties", H. Weinstock and M. Niseno (eds), *Microwave Superconductivity*, Kluwer Academic Publishers. Printed in the Netherlands, 2001.
- [10] [https://www.photonics.ethz.ch/fileadmin/user\\_upload/Courses/NanoOptics/nfoprobes\\_rev-1.pdf](https://www.photonics.ethz.ch/fileadmin/user_upload/Courses/NanoOptics/nfoprobes_rev-1.pdf)

- [11] Steven MA, Vladimir VT, Andrew RS, "Principles of Near-Field Microwave Microscopy", July 17, 2006. <http://citeseerx.ist.psu.edu/viewdoc/download?doi=10.1.1.569.1377&rep=rep1&type=pdf>
- [12] Schelkuno S, "Antennas, Theory and Practice". Wiley and Sons, Inc., New York, 1952.
- [13] Osofsky SS, Schwarz SE, "Design and performance of a noncontacting probe for measurements on high-frequency planar circuits", *IEEE Transactions on Microwave Theory and Techniques*, Vol. 40, No. 8, pp. 1701–1708, 1992.
- [14] Jean JB, Rémi C, "Image formation in near-field optics", *Progress in Surface Science*, Vol. 56, No. 3, pp. 133–237, 1997.
- [15] Alexander NR, "Quasistatics and electrodynamics of near-field microwave microscope", *Journal of Applied Physics*, Vol. 115, arct. no. 084501, 2014.
- [16] Björn TR, "High-frequency near-field microscopy", *Review of Scientific Instruments*, Vol. 73, No. 7, 2002.
- [17] Steinhauer DE, Vlahacos CP, Dutta SK, Wellstood FC, Steven MA, "Surface Resistance Imaging with a Scanning Near-Field Microwave Microscope", *Applied Physics Letters*, Vol. 71, pp. 1736, 1997. <http://arxiv.org/abs/cond-mat/9712142v1>
- [18] Lewis G, et al, "Apertureless scanning near-field optical microscopy: A comparison between homodyne and heterodyne approaches", *Journal of Optical Society B*, Vol. 23, May 2006.
- [19] Synge EH, "A suggested method for extending the microscopic resolution into the ultra-microscopic region". *Philosophical Magazine*, Vol. 6, pp. 356, 1928.
- [20] Bethe HA, "Theory of diffraction by small holes", *Physical Review*, Vol. 66, No. 7–8, pp. 163–182, 1944.
- [21] Bouwkamp CJ, "On the freely vibrating circular disk and the diffraction by circular disks and apertures", *Physica*, Vol. 16, No. 1, pp. 1–16, 1950.
- [22] Bouwkamp CJ, "Diffraction Theory", *Reports on Progress in Physics*, Vol. 17, 1954.
- [23] Massey GA, Davis JA, Katnik SM, Omon E, "Subwavelength resolution far-infrared microscopy", *Applied Optics*, Vol. 24, No. 10, pp. 1498–1501, 1985.
- [24] Grober RD, Rutherford T, Harris TD, "Modal approximation for the electromagnetic field of a near-field optical probe", *Applied Optics*, Vol. 35, No. 19, pp. 3488–3495, 1996.
- [25] Soohoo RF, "A microwave magnetic microscope", *Journal of Applied Physics*, Vol. 33, No. 3, pp. 1276–1277, 1962.
- [26] Ash EA, Nicholls G, "Super-resolution aperture scanning microscope", *Nature*, Vol. 237, No. 5357, pp. 510–512, 1972.
- [27] Bryant CA, Gunn JB, "Noncontact technique for the local measurement of semiconductor resistivity", *Review of Scientific Instruments*, Vol. 36, No. 11, pp. 1614–1617, 1965.

- [28] Pohl DW, Denk W, Lanz M, "Optical stethoscopy: Image recording with resolution  $\lambda/20$ ". *Applied Physics Letters*, Vol. 44, No. 7, pp. 651–653, 1984.
- [29] Betzig E, Isaacson M, Lewis A, "Collection mode near-field scanning optical microscopy", *Applied Physics Letters*, Vol. 51, No. 25, pp. 2088–2090, 1987.
- [30] Fee M, Steven C, Hänsch TW, "Scanning electromagnetic transmission line microscope with sub-wavelength resolution", *Optics Communications*, Vol. 69, No. 3–4, pp. 219–224, 1989.
- [31] Golosovsky M, Dan D, "Novel millimeter-wave near-field resistivity microscope", *Applied Physics Letters*, Vol. 68, No. 11, pp. 1579–1581, 1996.
- [32] Coptly A, Golosovsky M, Davidov D, Frenkel A, "Localized heating of biological media using a 1-W microwave near-field probe", *IEEE Transactions on Microwave Theory and Techniques*, Vol. 52, No. 8 II, pp. 1957–1963, 2004.
- [33] Bae J, Okamoto T, Fujii T, Mizuno K, Nozokido T, "Experimental demonstration for scanning near-field optical microscopy using a metal micro-slit probe at millimetre wavelengths", *Applied Physics Letters*, Vol. 71, No. 24, pp. 3581–3583, 1997.
- [34] Nozokido T, Iibuchi R, Bae J, Mizuno K, Kudo H, "Millimeter-wave scanning near-field anisotropy microscopy", *Review of Scientific Instruments*, Vol. 76, No. 3, art. no. 033702, 2005.
- [35] Nozokido T, Bae J, Koji M, "Scanning near-field millimeter-wave microscopy using a metal slit as a scanning probe", *IEEE Transactions on Microwave Theory and Techniques*, Vol. 49, No. 3, pp. 491–499, 2001.
- [36] Hunsche S, Koch M, Brener I, Nuss M, "THz near-field imaging", *Optical Communications*, Vol. 150, No. 22, 1998.
- [37] Mitrofanov O, et al. "Collection mode near field imaging with 0.5 THz pulses", *IEEE Journal of Selected Topics in Quantum Electronics*, Vol. 7, No. 4, pp. 630–640, 2001.
- [38] Mitrofanov O, et al. "Near field microscope probe for far infrared time domain measurements", *Applied Physics Letters*, Vol. 77, pp. 591–593, 2000.
- [39] Mitrofanov O et al. "Terahertz near field microscopy based on a collection mode detector", *Applied Physics Letters*, Vo. 77, pp. 3496–3498, 2000.
- [40] Wynne K, Carey J, Zawadzka J, Jaroszynski D, "Tunneling of single cycle terahertz pulses through waveguide", *Optical Communications*, Vo. 176, pp. 429–435, 2000.
- [41] Chen Q, Jiang Z, Xu G, Zhang XC, "Near field terahertz imaging with a dynamic aperture", *Optical Letters*, Vol. 25, p. 11222, 2000.
- [42] van der VN, Planken P, "Electro optic detection of sub wavelength terahertz spot sizes in the near field of a metal tip", *Applied Physics Letters*, Vol. 81, p. 1558, 2002.
- [43] Planken P, van der VN, "Spot size reduction in terahertz apertureless near field imaging", *Optical Letters*, Vol. 29, p. 2306, 2004.

- [44] Wang K, Barkan A, Mittleman B, "Propagation effects in aperture less near field optical antennas", *Applied Physics Letters*, Vol. 84, p. 305, 2004.
- [45] Chen HT, Kersting R, Cho G, "Terahertz imaging with nanometer resolution", *Applied Physics Letter*, Vol. 83, p. 3009, 2003.
- [46] George VE, Michael S, "Transforming Electromagnetics using Metamaterials", *IEEE magazine*, April, 2012.
- [47] Yuandan D, Tatsuo I, "Promising Future of Metamaterials", *IEEE magazine*, April, 2012.
- [48] Nathan BK, David RS, John BP, "Electromagnetic design with transformation optics", *Proceedings of the IEEE*, Vol. 99, No. 10, 2010.
- [49] Tie JC, David R, Smith RL, "Metamaterials Theory, Design and Applications", Springer, 2010.
- [50] Eroglu A, "Wave Propagation and Radiation in Gyrotropic and Anisotropic Media", DOI 10.1007/978-1-4419-6024-5\_2, Springer Science+Business Media, LLC, 2010.
- [51] Guven K, Ozbay E, "Near field imaging in microwave regime using double layer splitting resonator based metamaterial", *Opto-Electronics Review*, Vol. 14, No. 3, pp. 213–216, 2006.
- [52] Viktor GV, "The electrodynamics of substances with simultaneously negative values of  $\epsilon$  and  $\mu$ ", *Reviews of Topical Problems, Soviet Physics Uspekhi*, 1968.
- [53] Penday J, "Manipulating the near field with metamaterials", *Optics & Photonics News*, Sep. 2004.
- [54] Smith DR, Willie JP, Vier DC, Nemat-Nasser SC, Schultz S, "Composite medium with simultaneously negative permeability and permittivity", *Physical Review Letters*, Vol. 84, No. 18, 2000.
- [55] David RS, David S, Jack JM, Pavel K, Patrick R, "Partial focusing of radiation by a slab of indefinite media", *Applied Physics Letters*, Vol. 84, p. 2244, 2004.
- [56] Shen JT, Platzman PM, "Near field imaging with negative dielectric constant lenses", *Applied Physics Letters*, Vol. 80, p. 3286, 2002.
- [57] David RS, David S, Marshall R, Sheldon S, Ramakrishna SA, John BP, "Limitations on subdiffraction imaging with a negative refractive index slab", *Applied Physics Letters*, Vol. 82, p. 1506, 2003.
- [58] Lai A, Itoh T, Caloz C, "Composite right/left-handed transmission line metamaterials", *IEEE Microwave Magazine*, Vol. 5, No. 3, 2004.
- [59] David MP, "Microwave Engineering", 4th Edition, Wiley & Sons, 2012.
- [60] Yijun F, Xiaohua T, Yan C, Tian J, "Electromagnetic wave propagation in anisotropic metamaterials created by a set of periodic inductor-capacitor circuit networks", *Physics Review B*, Vol. 72, art. no. 245107, 2005.

- [61] Anthony G, George VE, "Overcoming the diffraction limit with a planar left-handed transmission-line lens", *Physics Review Letter*, Vol. 92, art. no. 117403, 18 March 2004.
- [62] Muhammed SB, Omar MR, "Experimental and numerical study of sensitivity improvement in near-field probes using single-negative media", *IEEE Transactions on Microwave Theory and Techniques*, Vol. 57, No. 12, pp. 3427–3433, 2009.
- [63] Stefan AM, Harry AA, "Plasmonics: Localization and guiding of electromagnetic energy in metal/dielectric structures", *Journal of Applied Physics*, Vol. 98, art. no. 011101, 2005.
- [64] Andrey KS, Vladimir MS, "Electrodynamics of Metamaterials", World Scientific Publishing Co. Pte. Ltd. 2007.
- [65] Ebbesen TW, Lezec HJ, Ghaemi HF, Thio T, Wolff PA, "Extraordinary optical transmission through sub-wavelength hole arrays", *Nature*, Vol. 391, pp. 667–669, 1998.
- [66] Dmitri KG, Sergey IB, "Plasmonics beyond the diffraction limit", *Nature Photonics*, Vol. 4, pp. 83–91, 2010.
- [67] Nicholas F, Hyesog L, Cheng S, Xiang Z, "Sub-diffraction-limited optical imaging with a silver superlens", *Science*, Vol. 308, p. 22, April 2005.
- [68] Megel et al. "Enhanced millimeter wave transmission through quasioptical subwavelength perforated plate", *IEEE Transaction on Microwave and Propagation*, Vol. 53, No. 6, pp. 2146–2154, 2006.
- [69] Pendry JB, Holden AJ, Robbins DJ, Stewart WJ, "Low frequency plasmons in thin-wire structures", *Journal of Physics: Condensed Matter*, Vol. 10, pp. 371–382, 1998.